Substituent Position Dictates the Intercalative DNA-Binding Mode for Anthracene-9,10-dione Antitumor Drugs†

Farial A. Tanious,‡ Terence C. Jenkins,§ Stephen Neidle,*,§ and W. David Wilson*,‡

Department of Chemistry and Laboratory for Chemical and Biological Sciences, Georgia State University, Atlanta, Georgia 30303, and Cancer Research Campaign Biomolecular Structure Unit, The Institute of Cancer Research, Sutton, Surrey SM2 5NG, U.K.

Received July 9, 1992; Revised Manuscript Received September 16, 1992

ABSTRACT: Molecular modeling studies [Islam, S. A., Neidle, S., Gandecha, B. M., Partridge, M., Patterson, L. H., & Brown, J. R. (1985) *J. Med. Chem. 28*, 857–864] have suggested that anthracene-9,10-dione (anthraquinone) derivatives substituted at the 1,4 and 1,8 positions with $-NH(CH_2)_2NH(CH_2CH_3)_2^+$ side chains intercalate with DNA with both substituents in the same groove (classical intercalation) while a similarly substituted 1,5 derivative intercalates in a threading mode with one side chain in each groove. Modeling studies also suggested that anthracene-9,10-dione (anthraquinone) derivatives substituted at the 2,6 positions with $-NHCO(CH_2)R$ (where R is a cationic group) should bind to DNA by the threading mode, and several such derivatives have been synthesized [Agbandjie, M., Jenkins, T. C., McKenna, R., Reszka, A., & Neidle, S. (1992) *J. Med. Chem. 35*, 1418–1429]. We have conducted stopped-flow kinetics association and dissociation experiments on the interaction of these anthraquinones with calf thymus DNA and with DNA polymers with alternating AT and GC base pairs to experimentally determine the binding mode and how the threading mode affects intercalation rates relative to similarly substituted classical intercalators. The binding modes, determined by analysis of relative rates, energies of activation, and effects of salt concentration on association and dissociation rate constants, agree completely with the modes predicted by molecular modeling methods. Association and dissociation rate constants for the threading mode are approximately a factor of 10 lower than constants for the classical intercalation mode, and the two modes, thus, have similar binding constants. Variations in rate constants for changes in cationic substituents at the 2 and 6 positions of the anthraquinone ring were surprisingly small. This series of compounds demonstrates that it is possible to design intercalators with very similar binding constants but with significantly different binding kinetics. The success of molecular modeling in correctly predicting the binding mode for all of the compounds indicates that modeling will be very useful in the design of other such intercalators as potential drug candidates.

It is now well established that the anthracycline class of antitumor antibiotics binds intercalatively to duplex DNA (Gale et al., 1981; Kersten et al., 1966; Das et al., 1974; Sinha et al., 1977; Brown, 1983; Waring, 1970; Plumbridge & Brown, 1979; Neidle & Sanderson, 1983; Arcamone, 1981; Quigley et al., 1980; Patel et al., 1981), and that intercalation is a necessary (though by itself insufficient) requirement for biological activity (Reszka et al., 1988). A number of totally synthetic anthracene-9,10-dione (anthraquinone) compounds have been developed in recent years, with the 1,4-bis(amino)-functionalized compound mitoxantrone now being in clinical use, particularly for the treatment of breast cancer (Stuart-Harris et al., 1984; Combleet et al., 1984; Alberts et al., 1988). The therapeutic success of this family of drugs and the closely related anthracycline agents has created considerable interest in the synthesis and study of new derivatives of this class.

We have been systematically studying the ramifications of both differing substituents on the anthracene-9,10-dione ring system and different substituent positions (Figure 1) on DNA interaction and the possible relationships to biological properties (Islam et al., 1985; Collier & Neidle, 1988; Agbandje et al., 1992). Molecular modeling studies have suggested that the symmetric 1,5-disubstituted series could bind to DNA by

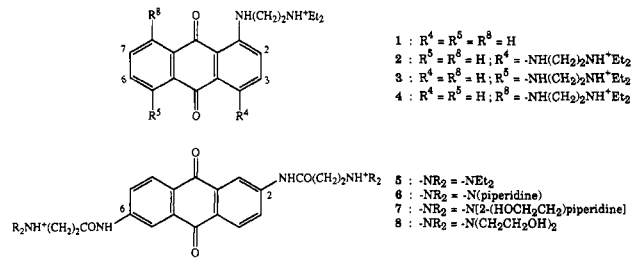

FIGURE 1: Structures of the anthracene-9,10-dione compounds.

a "threading"-type process, rather than via classic intercalation (Islam et al., 1985). This threading mode, for ligands with two bulky, distal-substituted side-chains, has been established on the basis of kinetic (Gabbay et al., 1973; Fox & Waring, 1984; Fox et al., 1985; Tanious et al., 1991), molecular modeling (Collier et al., 1984), X-ray crystallographic (Arora, 1983; Wang et al., 1990; Liaw et al., 1989; Williams et al., 1990), and NMR data (Searle et al., 1988; Zhang & Patel, 1990) for the anthracycline drug nogalamycin. Its essential feature is that the two side chains (or rings in the case of nogalamycin) lie one in each of the major and minor DNA grooves. This is in contrast to classic intercalators with substituent(s) lying in one or the other of the grooves, depending on their steric requirements.

There is necessarily some disturbance of the DNA structure in order to affect threading of a bulky polar side chain from one side of the DNA to the other. Two key features are

† This work was supported by NIH Grant AI-27196, the Cancer Research Campaign (U.K.), and NATO.

* To whom correspondence (either author) should be addressed.
‡ Georgia State University.
§ The Institute of Cancer Research.

0006-2960/92/0431-11632$03.00/0

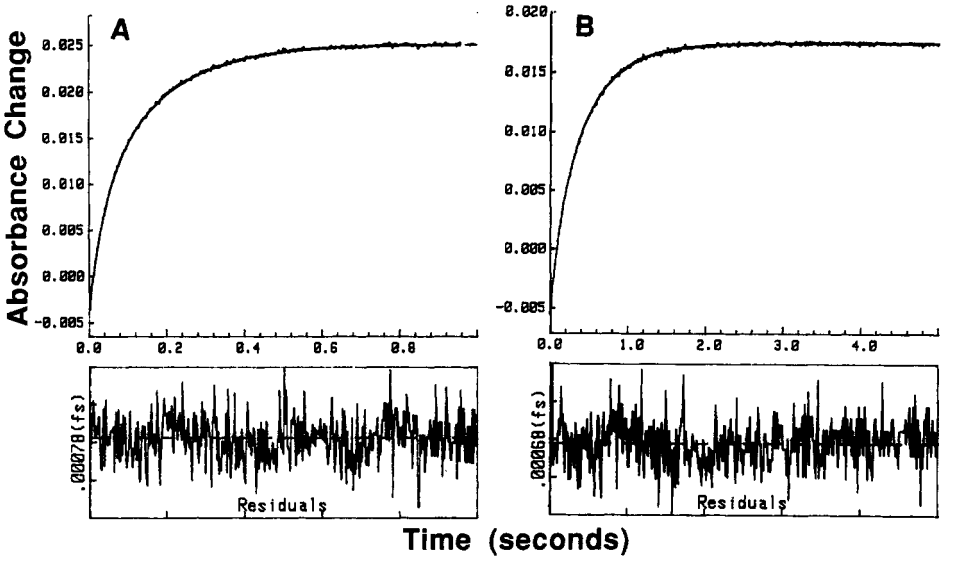

FIGURE 2: Stopped-flow kinetic traces for the SDS-driven dissociation of compounds **4** (A) and **5** (B) from calf thymus DNA. The experiments were conducted at 293 K in MES buffer with 0.1 M added salt at a ratio of 1:10 drug to DNA base pairs. The concentration of compound after mixing was 1×10^{-5} M. The smooth lines are the two-exponential fits to the data. Residual plots for the fits are shown under each experimental plot.

predicted for such a mechanism: (i) both the association and dissociation rate constants should be decreased relative to classical intercalative DNA binding and (ii) threading of cationic side chains (cf. the anthracene-9,10-diones in Figure 1) through the DNA duplex would require sequential formation and breakage of electrostatic interactions in the threading complex, and this can be detected through analysis of salt effects on rate constants (Wilson & Tanious, 1993). We have recently analyzed the association and dissociation kinetics of a series of naphthalene diimide intercalator compounds and have shown that their behavior is typical of DNA threading agents. Hence we have been able to define their general features of DNA complex formation, including a dependency upon ion concentration (Tanious et al., 1991).

We now extend this methodology to two groups of basic anthracene-9,10-dione derivatives: (i) a series of agents substituted at the 1, 1,4, 1,5, and 1,8 positions that have been predicted from molecular modeling studies to show diverse DNA intercalation behavior (Islam et al., 1983, 1985) and (ii) a novel series of symmetric 2,6-disubstituted compounds predicted to require a threading-type mechanism for intercalative binding to DNA (Neidle & Jenkins, 1991; Agbandje et al., 1992).

MATERIALS AND METHODS

Materials. Two groups of basic anthracene-9,10-diones compounds were studied: group I compounds **1–4** (Figure 1), which differ in the positions of ring substitution by basic moieties, i.e., 1-mono- and 1,4-, 1,5-, and 1,8-bis[2-(diethylamino)ethylamino]anthracene-9,10-diones, and group II compounds **5–8**, with varying basic 2,6-substituted amidoanthracene-9,10-diones. The synthesis and purification of these compounds have been reported previously (Islam et al., 1983, 1985; Agbandje et al., 1992). Calf thymus DNA (CT-DNA, Worthington), poly[dG-dC]$_2$ and poly[dA-dT]$_2$ (P-L Biochemicals) were prepared as previously described (Wilson et al., 1985b, 1986). Aqueous MES buffer contained 1×10^{-2} M 2-(*N*-morpholino)ethanesulfonic acid (MES) and 1×10^{-3} M EDTA. Sodium chloride was added to adjust the ionic strength to the desired value, as required, and the pH was adjusted to 6.2. Sodium dodecyl sulfate (SDS) was obtained from Boehringer Mannheim GmbH.

Methods. Kinetics measurements were conducted with a Hi-Tech SF-51 stopped-flow spectrophotometer. The software provided with the instrument was used for both data acquisition and analysis. Data acquisition was carried out via a 12-bit high-speed analog-to-digital converter in a HP-330 computer interfaced to the spectrophotometer. Single-wavelength kinetic records of absorbance versus time were collected. Typically, several individual kinetics experiments were collected and averaged by the computer to improve the signal-to-noise ratio. Dissociation reactions were monitored by mixing equal volumes (50 μL) of a solution of the DNA–drug complex with a 1% (w/w) solution of SDS at the same salt concentration. Association kinetic measurements were conducted under pseudo-first-order conditions by using excess DNA. Equal volumes (50 μL) of a DNA solution and a solution of compound were mixed. The temperature was controlled by circulating water with a Haake A81 refrigerated water bath and was monitored with an internal thermistor positioned in the SF-51 sample compartment.

RESULTS

Stopped-Flow Kinetics: Dissociation from CT-DNA. Stopped-flow SDS-driven dissociation kinetics were determined at 293 K for complexes of compounds **1–8** with CT-DNA in MES-buffered aqueous solution. Typical kinetic traces for the dissociation of complexes of **4** (group I) and **5** (group II) with CT-DNA are shown in Figure 2, where two-exponential best-fit curves to the data are shown along with plots of the residuals. There was a significant improvement, based on rms (root mean square) deviation and the distribution of the residuals, in fitting the experimental data to summed dual- rather than single-exponential curves under the conditions of these experiments. No significant improvement in either rms deviation or residuals was observed for a three-exponential fit. The two rate constants for the dual-exponential fits differ by a <4-fold factor (Table I), and hence, such similar processes can only be resolved under the high-resolution stopped-flow conditions illustrated in Figure 2. The amplitude for the fast phase of the interaction of these two compounds accounts for 25–40% of the total amplitude under all conditions used (Table I). To facilitate kinetics comparisons among compounds and comparisons of kinetics and equilibrium results

Table I: Dissociation Kinetics Results for Complexes of Compounds **1–8** with Calf Thymus DNA[a]

compound	k_1 (s^{-1})	A_1 (%)	k_2 (s^{-1})	A_2 (%)	τ(s)
		Group I			
1	150	87	68	13	0.007
2	9.5	55	1.8	45	0.17
3	2.5	15	0.74	85	1.0
4	25	37	6.2	63	0.08
		Group II			
5	6.2	28	2.1	72	0.31
6	8.4	38	2.1	62	0.22
7	8.6	32	1.5	68	0.27
8	12	22	2.5	78	0.22

[a] Experiments were conducted at 293 K in aqueous MES buffer containing 0.1 M added NaCl with a 1:10 molar ratio of drug to DNA (in base pairs).

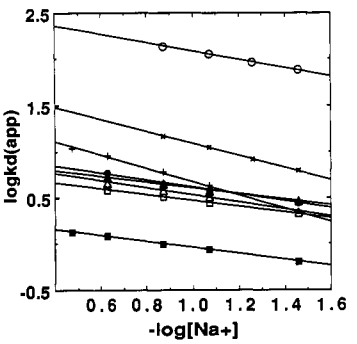

FIGURE 3: Plots of log k_d(app) vs –log [Na^+] for dissociation of compounds **1** (○), **2** (+), **3** (■), **4** (×), **5** (□), **6** (▲), **7** (△), and **8** (●) from calf thymus DNA. Experiments were conducted at 293 K in MES buffer at different ionic strengths in the manner described in Figure 2.

for the same compound, the dissociation lifietime (τ) and apparent rate constant for dissociation ($k_{app} = 1/\tau$) were calculated from the computer-derived best-fit values for the rate constants and amplitudes:

$$\tau = 1/(A_1k_1 + A_2k_2) \quad (1)$$

where the A and k values refer to the fractional amplitudes and rate constants, respectively, for the two-exponential components fitted to the data (Table I). The averaging procedure also removes problems of parameter correlation that can occur when fitting very similar overlapping smooth curves such as those obtained with these compounds.

The dissociation rate constants for the complexes of compounds **1–8** from CT-DNA were measured at several salt concentrations and plots of log k_d(app) as a function of –log [Na^+] are shown in Figure 3. Plots of log k_1 and log k_2 as a function of –log [Na^+] are more crowded but give the same slopes, within experimental error, as determined using the k_d(app) values. The slopes for SDS-driven dissociation of complexes with **1**, **3**, and **5–8** are 0.35 ± 0.05, while the corresponding values for compounds **2** and **4** are 0.65 and 0.73, respectively (Figure 3). Group I compounds have significantly different rates and slopes in this plot, while compounds from group II have more similar results.

Dissociation from CT-DNA: Effect of Temperature. Since Group I compounds exhibit such different behavior, dissociation experiments were conducted for the complexes of dications **2–4** with CT-DNA in MES buffer with 0.05 M added NaCl as a function of temperature. The apparent rate constant for these three compounds are shown in an Arrhenius plot in Figure 4S (supplementary material). Over the accessible temperature range, the dissociation of **3** from CT-DNA is always slower than the dissociation of both **2** and **4**. Activation enthalpies of 18 kcal mol^{-1} (compounds **2** and **4**) and 23 kcal mol^{-1} (compound **3**) for drug dissociation from the CT-DNA complexes were calculated from the plots (Figure 4S).

Table II: Comparison of Dissociation Results for Complexes of Compounds **2–5** and **8** with Polydeoxynucleotides[a]

	k_1 (s^{-1})		A_1 (%)		k_2 (s^{-1})		A_2 (%)		τ(s)	
drug	A-T	G-C	A-T	G-C	A-T	G-C	A-T	G-C	A-T	G-C
2	26	13	66	10	14	2.0	34	90	0.05	0.32
3	3.1	2.2	15	15	0.6	0.8	85	85	1.0	0.96
4	62	49	35	14	29	5.2	65	86	0.02	0.09
5	7.7	16	19	39	1.8	1.5	81	61	0.35	0.14
8	14	7.1	29	22	2.7	1.6	71	78	0.17	0.36

[a] Experiments were conducted at 293 K in aqueous MES buffer containing 0.1 M added NaCl with a 1:10 molar ratio of drug to polymer (in base pairs). A-T and G-C refer to poly(dA-dT)$_2$ and poly(dG-dC)$_2$, respectively.

Dissociation from Polynucleotides. The SDS-driven dissociation of representative compounds **2–5** and **8** from complexes with poly[dA-dT]$_2$ and poly[dG-dC]$_2$ were investigated (Table II) to determine how the dissociation varies with base-pair composition. As with CT-DNA, dissociation of all compounds from the polymers required dual-exponential fits to the experimental data. Group I compounds **2** and **4** dissociate more slowly from poly[dG-dC]$_2$ than from poly[dA-dT]$_2$ (Figure 5). Compound **3** has a similar lifetime with the A-T and G-C polymers but dissociates more slowly than either **2** or **4** from both polymers under the same conditions. In Group II, **5** has a longer lifetime by a ~2-fold factor for poly[dA-dT]$_2$ than from poly[dG-dC]$_2$ complexes, while **8** has a longer lifetime for complexes with poly[dG-dC]$_2$ than for the A-T polymer under the same conditions.

The dissociation rate constants for compounds **2–5** and **8** from the complexes formed with each polymer were also measured at several salt concentrations; plots of log k_d(app) as a function of –log [Na^+] are shown in Figure 6. For group I, the slopes for dissociation of compounds **2** and **4** are 0.70 ± 0.05 from poly[dA-dT]$_2$ and 0.74 ± 0.08 from poly[dG-dC]$_2$, while for compound **3** the corresponding values are 0.37 ± 0.05 and 0.43 ± 0.05, respectively. Dissociation rate constants for a naphthalene diimide threading intercalator (Tanious et al., 1991) are also shown in Figure 6A, where the determined slopes with the A-T and G-C polymers are 0.30 and 0.35, respectively. For group II, the slopes for complexes with **5** and **8** are 0.35 ± 0.05 (Figure 6B). For comparative purposes, dissociation rate constants for ethidium and propidium are also plotted in Figure 6B. With the A-T and G-C polymers the slopes determined for propidium and ethidium are 0.7–0.8 and 0.3–0.4, respectively (Figure 6B).

Stopped-Flow Kinetics: Association with CT-DNA. The association reaction of compound **1** with CT-DNA is fast and cannot be followed by stopped-flow techniques. The association reactions of compounds **2–8** with CT-DNA were measured as a function of DNA concentration at a salt concentration of [Na^+] = 0.2 M and with an approximately 10-fold molar excess of DNA (in terms of base pairs) over the ligand compound. Increasing the mole ratio of 20:1 to 30:1, at constant DNA concentration, had no significant effect on the rate constants for association, as expected for a pseudo-first-order reaction. Experimental traces of absorbance versus time are plotted under similar conditions in Figure 7 for the binding of **2** and **3** to CT-DNA. The association rate constant for the binding of **2** is significantly larger than that for binding of compound **3**. As with dissociation experiments, satisfactory

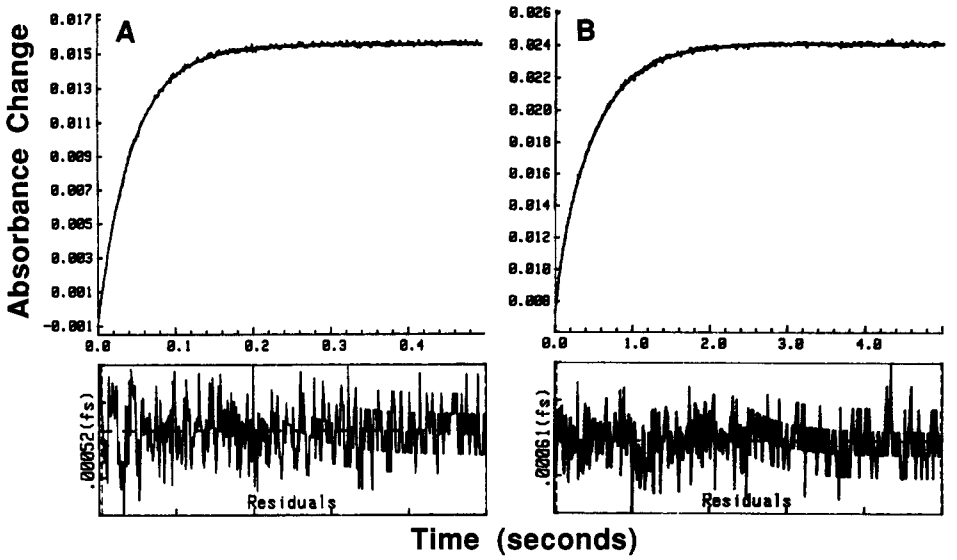

FIGURE 5: Stopped-flow kinetic traces for the SDS-driven dissociation of compound 2 (A) from poly[d(A-T)]$_2$, and (B) poly[d(G-C)]$_2$. The experiments were conducted at 293 K in MES buffer with 0.10 M added NaCl at a ratio of 1:10 compound to polymer base pairs. The concentration of the compounds after mixing was 1.0×10^{-5} M. The smooth lines are two-exponential fits to the experimental data. Residual plots are shown under each experimental plot.

fits to the experimental data were obtained with dual- rather than single-exponential curves (Figure 7). The differences in the two rate constants for the dual-exponential fits involve a factor of 2–3 and k_a(app) values were calculated by using eq 1.

Apparent association rate constants can be fitted to eq 2 over DNA concentrations of (1–25) $\times 10^{-5}$ M:

$$k_a(\text{app}) = k_a[\text{DNA}] + k_d \qquad (2)$$

where [DNA] is the molar concentration of DNA in base pairs, k_a(app) is the apparent pseudo-first-order association rate constant at each DNA concentration, k_a is the intrinsic second-order association rate constant, and k_d is the first-order dissociation rate constant for the DNA–drug complex. Experiments such as those shown in Figure 7 were repeated at a range of DNA concentrations for compounds **2–8** to determine the second-order association rate constants (k_a) according to eq 2 (Figure 8S, supplementary material). The plots are linear within experimental error (Figure 8S), and the slope of the line gives the second-order association rate constant, while the intercept gives the calculated dissociation rate constant for these conditions. For comparative purposes, association rate constants for propidium in 0.2 M NaCl are also plotted in Figure 8S. The experiments were also conducted at several salt concentrations for association of compounds **2** and **3** (Figure 9S, supplementary material) and log k_a versus log [Na^+] plots are shown in Figure 10S (supplementary material). As can be seen, the k_a value for association of compound **3** with CT-DNA has a very high salt dependence, while the k_a value for association of **2** with CT-DNA has a lower salt dependence. The rate constants for association of compounds **3** and **5–8** to CT-DNA under the same conditions are typically $\sim 10^5$ M^{-1} s^{-1}, while the values determined for compounds **2**, **4**, and propidium are $\sim 10^6$ M^{-1} s^{-1} (Table III) even though all compounds are dications.

The measured dissociation rate constants for all compounds from CT-DNA, are in good agreement with the k_d value from eq 2 (Table III). We have previously found that the observed pseudo-first-order association rate constants for ethidium, propidium, and naphthalene diimide are also linear with respect to DNA concentration (Wilson et al., 1985a,b, 1986; Tanious et al., 1991).

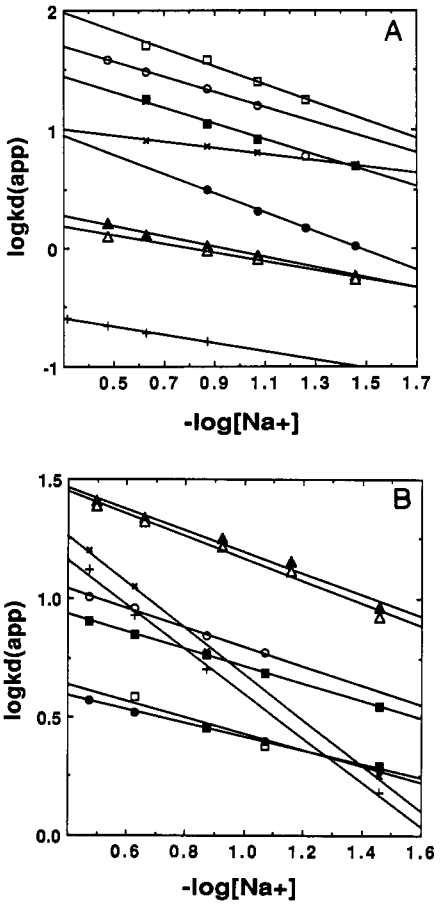

FIGURE 6: (A) Plots of log k_d(app) vs –log [Na^+] for dissociation of compounds **2** from poly[dA-dT]$_2$ (○) and poly[dG-dC]$_2$ (●), **3** from poly[dA-dT]$_2$ (△) and poly[dG-dC]$_2$ (▲), **4** from poly[dA-dT]$_2$ (□) and poly[dG-dC]$_2$ (■), and naphthalene diimide from poly[dA-dT]$_2$ (×) and poly[dG-dC]$_2$ (+). Experiments were conducted at 293 K in MES buffer in different ionic strengths in the manner described in Figure 5. (B) Plots of log k_d(app) vs –log [Na^+] for dissociation of compounds **5** from poly[dA-dT]$_2$ (●) and poly[dG-dC]$_2$ (○), **8** from poly[dA-dT]$_2$ (■) and poly[dG-dC]$_2$ (□), ethidium from poly-[dA-dT]$_2$ (▲) and poly[dG-dC]$_2$ (△), and propidium from poly-[dA-dT]$_2$ (×) and poly[dG-dC]$_2$ (+). Experiments were conducted in MES buffer at 293 K in different ionic strengths in the manner described in Figure 5.

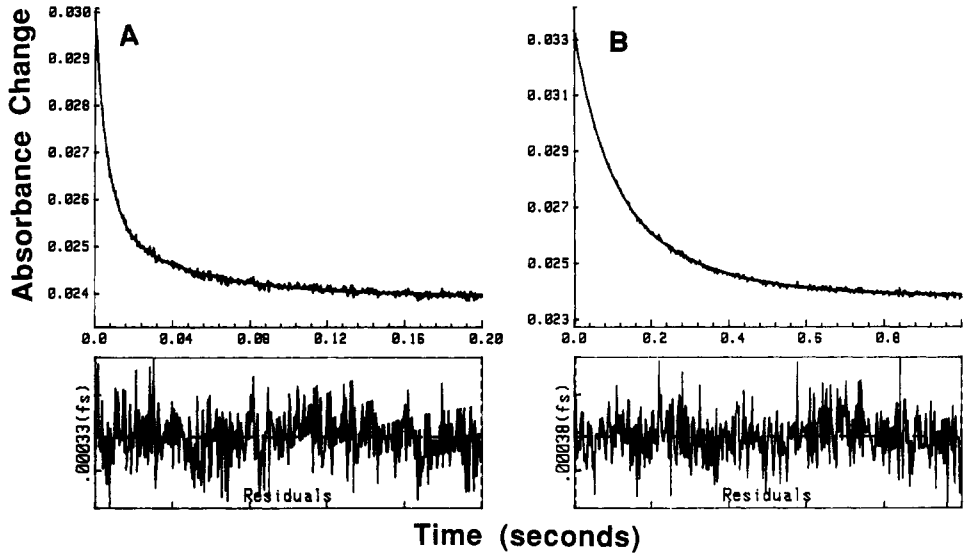

FIGURE 7: Stopped-flow kinetics association reactions for compounds **2** (A) and **3** (B) with calf thymus DNA. The total concentrations after mixing were 4.0×10^{-5} M for DNA (base pairs) and 4.0×10^{-6} M for the compounds in MES buffer with 0.20 M added NaCl at 293 K. The smooth lines are the two-exponential fits to the experimental data. Residuals plots are shown under each experimental plot.

Table III: Kinetic Constants and DNA Binding Constants for Compounds with Calf Thymus DNA

compound	$10^{-5}k_a$[a] (M^{-1} s^{-1})	k_d[b] (s^{-1})	k_d slope[b]	k_d[a] (s^{-1})	log K kinetic	log K equilibrium[c]
1	*d*	~200	0.44			5.6
2	24	8.9	0.73	10.7	5.4	5.4
3	2.1	1.2	0.34	0.93	5.4	5.3
4	7.0	19	0.65	18	4.6	5.0
5	1.5	3.8	0.32	3.2	4.7	
6	1.7	5.2	0.32	4.2	4.6	
7	1.1	4.6	0.39	2.1	4.7	
8	2.3	5.9	0.39	2.4	4.7	
propidium[e]	10.6	9.0	0.85	6.7	5.2	5.5
ethidium[e]	*d*	16.5	0.31			

[a] k_a and k_d values are from the slopes and intercepts of Figure 8S. [b] k_d from experimental data and slopes from Figure 3. [c] K values determined in 0.05 M NaCl (Islam et al., 1985) were converted to 0.2 M Na^+ using the equation $\partial \log K_{obs}/\partial \log[Na^+] = -m\psi$ (Record et al., 1976). [d] Too fast. [e] Data taken from Wilson et al. (1985).

Association with Polymers. As with CT-DNA the association reactions of compounds **3–5** and **8** with poly[dA-dT]$_2$ and poly[dG-dC]$_2$ were measured as a function of DNA concentration and at a salt concentration of $[Na^+] = 0.2$ M. Experimental traces of absorbance versus time are plotted under similar conditions in Figure 11 for binding of compound **3** to poly[dA-dT]$_2$ and poly[dG-dC]$_2$. As with the dissociation experiments, satisfactory fits were obtained with dual- rather than single-exponential fitted curves. The differences in the two rate constants for the two components of each fit were 2–3 and k_a(app) values were calculated with eq 1. Experiments such as those shown in Figure 11 were repeated at a range of DNA concentrations to determine the second-order association rate constant according to eq 2 (Figure 12S, supplementary material). The association rate constants for the binding of **3–5** and **8** to poly[dA-dT]$_2$ are significantly larger than those for poly[dG-dC]$_2$ (Table IV). The rate constants (k_a) for association for these compounds to A-T and G-C polynucleotides are collected in Table IV. The measured dissociation rate constants for these compounds from both ligand–polymer complexes are in good agreement with the k_d values calculated from eq 2 (Table IV).

DISCUSSION

A number of solution experiments, supported by molecular modeling studies, have shown that the anthracene-9,10-diones **1–8** bind to DNA by intercalation (Islam et al., 1985; Neidle & Jenkins, 1991; Agbandje et al., 1992). Two quite different types of intercalation complexes of the disubstituted anthracene-9,10-dione compounds with DNA are possible: (i) complexes with one side chain in each groove (threading) and (ii) more classical intercalation complexes with the two side chains lying in the *same* groove. In the threading model, one polar side chain must pass between base pairs during intercalation, and this significantly slows the rates of both ligand association and dissociation. With both classical and threading intercalators the rate constants and their dependence on salt concentration vary with the binding mode, and kinetic studies thus offer a direct method for accurate determination of binding mode (Wilson et al., 1985a, 1989, 1990a–c; Tanious et al., 1991).

Compound **1** has very fast association and dissociation rates and a log k_d vs –log $[Na^+]$ slope value of 0.4 for dissociation from calf thymus DNA, in accord with the behavior expected for a simple monocationic intercalator on the basis of comparisons with known intercalators such as ethidium (Wilson et al., 1985a). The disubstituted anthracene-9,10-dione compounds **2–8** are dications and exhibit more complicated kinetic behavior and complex conformations. Results for these ligands will be compared to those for naphthalene diimide and propidium, an established threading intercalator and a "classical" DNA intercalator, respectively (Waring,

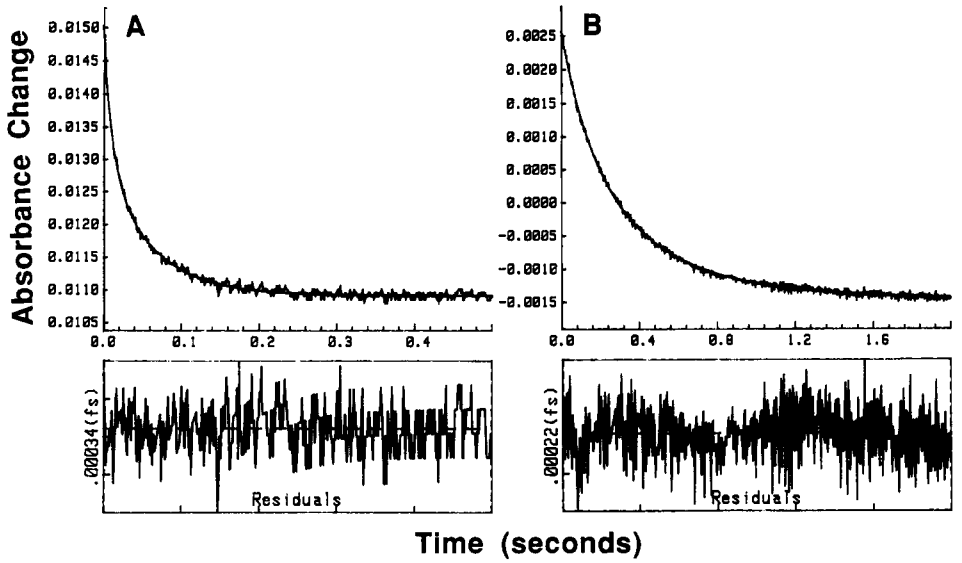

FIGURE 11: Stopped-flow kinetics association reactions for compound **3** (A) with poly[dA-dT]$_2$ and (B) poly[dG-dC]$_2$. The total concentrations after mixing were 2.0×10^{-5} M for DNA (base pairs) and 2.0×10^{-6} M for the compounds in MES buffer with 0.20 M added NaCl at 293 K. The smooth lines are the two-exponential fits to the experimental data. Residuals plots are shown under each experimental plot.

Table IV: Polymer Complex Kinetic Constants and Calculated Kinetic DNA Binding Constants[a]

	$10^{-5}k_a$[b] (M^{-1} s^{-1})		k_d[c] (s^{-1})		k_d slope[c]		k'_d[b] (s^{-1})		log K'/log K[d]	
compound	A-T	G-C	A-T	G-C	A-T	G-C	A-T	G-C	A-T	G-C
2	*e*	18.9	30.4	6.0	0.64	0.81		9.3		5.3/5.5
3	22	1.5	1.1	1.3	0.37	0.44	3.3	1.3	5.8/6.3	5.1/5.1
4	71	3.9	51	15	0.74	0.66	57.5	7.6	5.1/5.1	4.7/4.4
5	12.2	0.92	3.5	9.2	0.30	0.41	3.5	4.7	5.5/5.5	4.3/4.0
8	15.1	3.2	7.7	3.0	0.37	0.35	13.9	2.3	5.0/5.3	5.1/5.0
naphthalene diimide[f]	3.4	1.4	8.3	0.2	0.26	0.35	7.4	0.21	4.7/4.6	5.8/5.9
propidium[f]	12.8		11.2	8.5	0.97	0.95	9.03		5.2/5.1	
ethidium[f]			22	21	0.45	0.47				

[a] A-T and G-C refer to poly(dA-dT) and poly(dG-dC) oligonucleotide duplexes, respectively. [b] k_a and k'_d values are from the slopes and intercepts in Figure 12S. [c] k_d values are from dissociation experiments in 0.2 M NaCl and the slopes from Figure 6. [d] K' and K values calculated from k_a/k'_d and k_a/k_d, respectively, in 0.2 M NaCl. [e] Too fast. [f] Data taken from Tanious et al. (1991) and Wilson et al. (1985b).

1970; Yen et al., 1982; Wilson et al., 1985a; Tanious et al., 1991).

Group I Dications. With CT-DNA compound **2** has a log k_d(app) vs –log [Na^+] slope that is very similar to the propidium slope and rate constants for association and dissociation that are ~2-fold greater than the propidium values. Similar results for dissociation of **2** from CT-DNA at a fixed set of conditions have been obtained by Denny and Wakelin (1990). The association and dissociation rate constants for poly[dA-dT]$_2$ complexes of **2** are larger than for poly[dG-dC]$_2$ complexes, but the polymer complexes have similar log k_d(app) vs –log [Na^+] slopes that are in turn similar to the propidium value. The slopes are approximately twice the value observed with the naphthalene diimide threading intercalator. These results indicate that **2** binds to all DNA sequences with both side chains in the same groove, as has been suggested for mitoxantrone (Collier et al., 1984; Lown & Hanstock, 1985) and as predicted by modeling studies (Islam et al., 1983). With both side chains in the same groove, the anthracene-9,10-dione chromophore must be oriented approximately perpendicular to the base-pair long axes as observed in crystallographic structures for DNA oligonucleotides complexes of daunomycin (for example, Wang et al., 1987; Frederick et al., 1990). All 1,4-disubstituted anthracene-9,-10-dione derivatives that have been studied to this time exhibit this general type of binding mode.

Compound **3** has association and dissociation rate constants for its CT-DNA complex that are >10-fold slower than with **2** (Table III). The k_d(app) versus –log [Na^+] slope with **3** is approximately half that for **2** and is more similar to the slope for the naphthalene diimide threading intercalator. With the polymers (Table IV) the rate constants for **3** in its complexes with poly[dA-dT]$_2$ are decreased more than for complexes with poly[dG-dC]$_2$ when compared to complexes of **2**. The dissociation rate constants are reduced more than the association constants and **3**, thus, has a slight AT-binding selectivity (Table IV). Both the significantly reduced rate constants and the k_d(app) vs –log [Na^+] slopes indicate that **3** binds to all DNA sequences by a threading intercalation mode as predicted for this compound by modeling studies (Islam et al., 1983, 1985). Unlike **2**, the chromophore of **3** must be approximately parallel to the long axes of the base pairs at the intercalation site in order to fit the cationic groups into opposite DNA grooves.

The CT-DNA association and dissociation rate constants for **4** are significantly greater than those for **3**. The association constant is not as large as for the **2** complex while the dissociation constant is larger, and **4** has a lower binding constant than either **2** or **3** (Table III). The k_d(app) vs –log [Na^+] slopes for **4** with both CT-DNA and with polymers are close to the values for **2** and propidium. The increased rate constants and slopes for **4**, relative to **3**, thus indicate that **4** binds to DNA with both cationic groups in the same groove, as with **2**. It should be noted, however, that the conformation of the **4** complex must be quite different than that with **2**. As noted above, the aromatic chromophore of **2** must be

approximately perpendicular to the long axes of the base pairs at the intercalation site, while for both side chains of **4** to fit in the same DNA groove requires the aromatic chromophore to be approximately parallel to this axis. Although the equilibrium constants of **4** with the A-T and G-C polymers are similar (Table IV), the rates for both association and dissociation are significantly faster with the A-T than with the G-C polymers. Optimum positioning of the two side chains of **4** within an intercalation site may require local motions that are faster at an A-T intercalation site than at an equivalent G-C binding site.

Moving one side chain of the disubstituted anthracene-9,10-diones **2**–**4** around the ring system thus yields three intercalators that bind to DNA in complexes with quite different conformations. It is interesting that **2** and **4**, which bind to DNA with both side chains in the same groove, have association and dissociation rate constants that are significantly larger with A-T than with G-C sequences. Compound **3** has a binding selectivity for A-T, and this clearly reduces its dissociation constant from A-T base pairs. As with **2** and **4**, the association rate constant for **3** with the A-T polymer is >10-fold higher than with poly[dG-dC]$_2$.

Group II Dications. Four compounds, disubstituted at the anthracene-9,10-dione 2,6 ring positions with significantly different substituents, were studied (Figure 1). With CT-DNA the compounds have quite similar dissociation rate constants and k_d(app) vs –log [Na^+] slopes (Figure 3). Although the differences are generally small, **5** has the smallest and **8** has the largest k_d value of the group II compounds, and for this reason, complexes of these two compounds were investigated with DNA polymers.

It is interesting that **5** has a larger k_d value with poly[dG-dC]$_2$ than with poly[dA-dT]$_2$ while **8** has a larger k_d value with the A-T polymer than with the G-C polymer (Table III). With both compounds the association rate constants are significantly larger with poly[dA-dT]$_2$. This combination of rate constants results in essentially nonspecific binding of **8** but AT-binding specificity for **5**.

The k_d(app) vs –log [Na^+] slopes for all group II compounds with CT-DNA and with the A-T and G-C polymers are in the 0.3–0.4 range, as expected for a threading intercalation mode for dications. The association rates for group II compounds are also lower than for classical intercalators and more similar to values with threading intercalators. Group II compounds thus bind to all DNA sequences by a threading binding mode in agreement with molecular modeling results (Neidle & Jenkins, 1991; Agbandje et al., 1992).

As has been observed with other intercalators, the compounds in both groups I and II require two-exponential curves to adequately fit the experimental results for dissociation and association reactions with natural and synthetic polymers DNAs. The two constants for any compound are not widely different, with the k_1/k_2 ratios typically in the 2–6 range with CT-DNA (Table I) and 2–10 with DNA polymers (Table II). Single-exponential fits to the results have a clear asymmetry in the residuals while three-exponential fits do not significantly improve either the residuals or the correlation coefficient for the fit. The two-exponential fits may represent two major families of closely related intercalation processes, but it is not clear, at present, what these two processes represent. An attractive possibility is that the two rates are for intercalation binding mechanisms from either the major or the minor groove directions. Since the 1,8-disubstituted compound **4** cannot easily intercalate from the minor-groove side for steric reasons but also requires two-exponential fit, the major–minor groove mechanism does not appear able to explain effects for all compounds. A second possibility is that the two components represent binding at different classes of sites, such as 5′-purine–pyrimidine or 5′-pyrimidine–purine. Such a proposal can explain the two-exponential fits for the polymers but is not as attractive for CT-DNA. However, 5′-purine–purine (or, equivalently, 5′-pyrimidine–pyrimidine) sites, particularly 5′-ApA, are generally disfavored for intercalation. Hence, from a mechanistic basis, it is possible that intercalation of the anthracene-9,10-diones into CT-DNA can be grouped into two families with similar rates, representing the purine–pyrimidine and pyrimidine–purine binding site classes. The smooth kinetic curves observed for dissociation and association would thus not allow additional resolution of the reaction families site individual components. With other intercalators the individual rates could be more different and, thus, could be resolved.

CONCLUSIONS

We have shown that the binding modes for the anthracene-9,10-diones in this paper involve threading-type intercalation for the 1,5- or 2,6-disubstituted compounds **3** and **5**–**8** and classical DNA intercalation for the 1,4- and 1,8-difunctionalized derivatives, **2** and **4**, where both side chains necessarily occupy the same groove. These findings thus provide an experimental basis for the binding modes suggested by molecular modeling studies. We note that compound **5** is markedly more active in a L1210 in vitro tumor cell line than **8** (Agbandje et al., 1992); it is tempting to speculate that this is related to the DNA base selectivity shown by **5**. The kinetics results in Table III indicate that classical intercalators (including propidium) have association rate constants in the $\geq 10^6\ M^{-1}\ s^{-1}$ range while threading intercalators have constants in the $\leq 2 \times 10^5\ M^{-1}\ s^{-1}$ range. The dissociation rate constants are $\sim 10\ s^{-1}$ or greater for classical intercalators but only ≤ 5–$6\ s^{-1}$ for threading intercalators. Compensating effects in changes for the association and dissociation rate constants lead to binding constants for classical and threading intercalators being closer than the kinetic constants.

The slow kinetics of association and dissociation of threading intercalators can be attributed to several features that depend on the intercalator structure and on the nucleic acid sequence. First, the polar/charged side chain must pass from solution through the more nonpolar region between base pairs in the duplex. Second, the steric size and rigidity of the side chains can be important. Third, the rate at which DNA can open to form intercalation sites or larger open conformations (a bubble-type structure) to accommodate large side chain dynamics can become essential for large threading intercalators. Cationic alkylamine side chains, such as on the anthraquinone derivatives in Figure 1, can assume extended configurations that will allow them to slide through a normal intercalation site. The slow kinetics of threading could then be due to an orientational factor that requires the side chains to be in a limited range of its total conformational space for intercalation. The resistance of the charged side chain to enter the relatively nonpolar region between base pairs could also serve to reduce reaction rates for threading intercalators. For threading intercalators with very large and rigid side chains, the normal intercalation site size would not allow the side chain to pass through to the opposite groove. In this case intercalation could only occur when slow thermal motions of the duplex produce a large opening that could arise, for example, by concerted opening of an intercalation site and breaking/breathing of one of the base pairs at the site.

A large difference is observed in association rate constants between the A-T and G-C polymers, but this difference is seen with both classical and threading intercalators (Denny & Wakelin, 1990; Wakelin, 1990) and is clearly not related in any simple manner to the binding mode. The energy of activation for dissociation of the threading intercalator **3** from CT-DNA is 23 kcal mol^{-1} while the energy of activation for the classical intercalators **2** and **4** is approximately 18 kcal mol^{-1}. The greater energy of activation for **3** contains terms for the additional distortion of DNA required for passing of a polar side chain between base pairs, as well as possible terms for side-chain distortion and desolvation. Even with these terms, association and dissociation rate constants for the threading intercalators of this work are significantly larger than for the threading antibiotic nogalamycin (Fox & Waring, 1984; Fox et al., 1985). The groups of the nogalamycin that must thread between base pairs for intercalation are more rigid than the side chains of **1–8** and must require additional distortion of DNA in the binding mechanism. It is possible that synthetic threading intercalators with such slow DNA binding kinetics could inhibit DNA-associated enzymes and, thus, exhibit new types of pharmacological activities. We are continuing molecular modeling and design studies of threading intercalators with the goal of preparing new DNA-interactive compounds and potential drugs.

ACKNOWLEDGMENT

We thank Mr. A. P. Reszka (ICR) for excellent technical assistance.

SUPPLEMENTARY MATERIAL AVAILABLE

Five figures showing Arrhenius plot [$\ln k_d$(app) versus $1/T$] for SDS-driven dissociation of **2**, **3**, and **4** from the complexes formed with calf thymus DNA (Figure 4S), plots of k_a(app) as function of calf thymus DNA concentration (in base pairs) for the association reactions of **2–8** and propidium (Figure 8S), observed pseudo-first-order association rate constants plotted as a function of calf thymus DNA concentration (in base pairs) for **2** and **3** in different Na^+ concentrations (Figure 9S), plots of log k_a(app) versus –log [Na^+] for association of **2**, **3**, and propidium with calf thymus DNA (Figure 10S), and plots of k_a(app) as a function of polymer concentration in base pairs for association reactions of **3**, **5**, and **8** with poly-[d(A-T)]$_2$ and poly[d(G-C)]$_2$ (Figure 12S) (5 pages). Ordering information is given on any current masthead page.

REFERENCES

Agbandjie, M., Jenkins, T. C., McKenna, R., Reszka, A., & Neidle, S. (1992) *J. Med. Chem. 35*, 1418–1429.

Alberts, D. S., Surwit, E. A., Peng, Y.-M., et al. (1988) *Cancer Research 48*, 5874–5877.

Arcamone, F. (1981) in *Doxorubicin, Anticancer Antibiotics* (Crooke, S. T., & Reich, S. D., Eds) Medicinal Chemistry 17, Academic Press, New York.

Arora, S. K. (1983) *J. Am. Chem. Soc. 105*, 1328–1332.

Brown, J. R. (1983) in *Molecular Aspects of Anti-Cancer Drug Action* (Neidle, S., & Waring, M. J., Eds), pp 57–92, Macmillan, London.

Collier, D. A., & Neidle, S. (1988) *J. Med. Chem. 31*, 847–857.

Collier, D. A., Neidle, S., & Brown, J. R. (1984) *Biochem. Pharmacol. 33*, 2877–2880.

Combleet, M. A., Stuart-Harris, R. C., Smith, I. E., Colman, R. E., Rubers, R. D., & Mouridsen, M. T. (1984) *Eur. J. Cancer Clin. Oncol. 20*, 1141–1146.

Das, G. C., Dasgupta, S., & Das Gupta, N. N. (1974) *Biochim. Biophys. Acta 353*, 274–282.

Denny, W. A., & Wakelin, L. P. G. (1990) *Anti-Cancer Drug Des. 5*, 189–200.

Fox, K. R., & Waring, M. J. (1984) *Biochim. Biophys. Acta 802*, 162–168.

Fox, K. R., Brassett, C., & Waring, M. J. (1985) *Biochim. Biophys. Acta 840*, 383–392.

Frederick, C. A., Williams, L. D., Ughetto, G., van der Marel, G. A., van Boom, J. H., Rich, A., & Wang, A. H.-J. (1990) *Biochemistry 29*, 2538–2549.

Gabbay, E. J., DeStefano, R., & Baxter, C. S. (1973) *Biochim. Biophys. Res. Commun. 51*, 1083–1089.

Gale, E. F., Cundiffe, E., Reynolds, P. E., Richmond, M. H., & Waring, M. J. (1981) *The Molecular Basis of Antibiotic Action*, 2nd ed., pp 258–401, Wiley, London.

Islam, S. A., Neidle, S., Gandecha, B. M., & Brown, J. R. (1983) *Biochem. Pharmacol. 32*, 2801–2808.

Islam, S. A., Neidle, S., Gandecha, B. M., Partridge, M., Patterson, L. H., & Brown, J. R. (1985) *J. Med. Chem. 28*, 857–864.

Kersten, W., Kersten, H., & Szybalski, W. (1966) *Biochemistry 5*, 236–244.

Liaw, Y.-C., Gao, Y.-G., Robinson, H., van der Marel, G. A., van Boom, J. H., & Wang, A. H.-J. (1989) *Biochemistry 28*, 9913–9918.

Lown, J. W., & Hanstock, C. C. (1985) *J. Biomol. Struct. Dyn. 2*, 1097–1106.

Neidle, S., & Jenkins, T. C. (1991) *Methods Enzymol. 203*, 433–458.

Neidle, S., & Sanderson, M. R. (1983) in *Topics in Molecular and Structural Biology* (Neidle, S., & Waring, M. J., Eds) Vol. 3, p 35, Macmillan Press, London.

Patel, D. I., Sozlowski, S. A., & Rich, A. (1981) *Proc. Natl. Acad. Sci. U.S.A. 78*, 3333–3337.

Plumbridge, R. W., & Brown, J. R. (1979) *Biochem. Pharmacol. 28*, 3231–3234.

Quigley, G. J., Wang, A. H.-J., Ughetto, G., van der Marel, G., van Boom, J. H., & Rich, A. (1980) *Proc. Natl. Acad. Sci. U.S.A. 77*, 7204–7208.

Record, M. T., Jr., Lohman, T. M., & DeHaseth, P. (1976) *J. Mol. Biol. 107*, 145–158.

Reszka, K., Kolodziejczyk, P., Hartley, J. A., Wilson, W. D., & Lown, J. W. (1988) in *Anthracycline and Anthracenedione-based Anticancer Agents* (Lown, J. W., Ed.), pp 401–405, Elsevier, Amsterdam.

Searle, M. S., Hall, J. G., Denny, W. A., & Wakelin, L. P. G. (1988) *Biochemistry 27*, 4340–4349.

Sinha, R. K., Talapatra, P., Mitra, A., & Mazumder, S. (1977) *Biochim. Biophys. Acta 474*, 199–209.

Stuart-Harris, R. C., Bozek, T., Pavlidia, N. A., & Smith, I. E. (1984) *Cancer Chemother. Pharmacol. 12*, 1–4.

Tanious, F. A., Yen, S. F., & Wilson, W. D. (1991) *Biochemistry 30*, 1813–1819.

Wakelin, L. P. G., Chetcuti, P., & Denny, W. A. (1990) *J. Med. Chem. 33*, 2039–2044.

Wang, A. H. J., Ughetto, G., Quigley, G. J., & Rich, A. (1987) *Biochemistry 26*, 1152–1163.

Wang, A. H.-J., Liaw, Y.-C., Robinson, H., & Gao, Y.-G. (1990) in *Molecular Basis of Specificity in Nucleic Acid–Drug Interactions* (Pullman, B., & Jortner, J., Eds.) Jerusalem Symposia on Quantum Chemistry and Biochemistry, Vol. 23, pp 1–21, Kluwer Academic Publishers, Dordrecht, The Netherlands.

Waring, M. J. (1970) *J. Mol. Biol. 54*, 247–279.

Williams, L. D., Egli, M., Gao, Q., Bash, P., van der Marel, G. A., van Boom, J. H., Rich, A., & Frederick, C. A. (1990) *Proc. Natl. Acad. Sci. U.S.A. 87*, 2225–2229.

Wilson, W. D., Krishnaoorthy, C. R., Wang, Y. H., & Smith, J. C. (1985a) *Biopolymers 24*, 1941–1961.

Wilson, W. D., Wang, Y. H., Krishnamoorthy, C. R., & Smith, J. C. (1985b) *Biochemistry 24*, 3991–3999.

Wilson, W. D., Wang, Y. H., Krishnamoorthy, C. R., & Smith, J. C. (1986) *Chem.-Biol. Interact. 58*, 41–57.

Wilson, W. D., Tanious, F. A., Barton, H. J., Strekowski, L., Boykin, D. W., & Jones, R. L. (1989) *J. Am. Chem. Soc. 111*, 5008–5010.

Wilson, W. D., Tanious, F. A., Barton, H. J., Jones, R. L., Fox, K., Wydra, R. L., & Strekowski, L. (1990a) *Biochemistry 29*, 8452–8461.

Wilson, W. D., Tanious, F. A., Barton, H. J., Wydra, R. L., Jones, R. L., Boykin, D. W., & Strekowski, L. (1990b) *Anti-Cancer Drug Des. 5*, 31–42.

Wilson, W. D., Tanious, F. A., Buczak, H., Venkatramanan, M. K., Das, B. P., & Boykin, D. W. (1990c) in *Molecular Basis of Specificity in Nucleic Acid–Drug Interactions* (Pullman, B., & Jortner, J., Eds.) Jerusalem Symposia on Quantum Chemistry and Biochemistry, Vol. 23, pp 331–352, Kluwer Academic Publishers, Dordrecht, The Netherlands.

Wilson, W. D., & Tanious, F. A. (1993) in *Molecular Aspects of Anticancer Drug–DNA Interactions* (Neidle, S., & Waring, M. J., Eds.) Macmillan Press, Riverside, NJ (in press).

Yen, S. F., Gabbay, E. J., & Wilson, W. D. (1982) *Biochemistry 21*, 2070–2076.

Zhang, X., & Patel, D. J. (1990) *Biochemistry 29*, 9451–9466.